Detection and Evaluation of Hydrogen Bond Strength in Nucleic Acid Base Pairs

Afshan Mohajeri* and Fatemeh Fadaei Nobandegani

Department of Chemistry, College of Sciences, Shiraz University, Shiraz 71454, Iran

Received: July 29, 2007; In Final Form: October 1, 2007

The strengths of N−H---N and N−H---O hydrogen bonds in 15 nucleic acid base pairs have been investigated using different descriptors. Geometrical and energetic criteria, atoms in molecules topological parameters, natural bond orbital analysis, and spectroscopic measurements have been used to detect the H-bonds and evaluate their strengths in the intermolecular interactions between five nucleic acid bases. Different correlations have been obtained between many of these descriptors to provide a global view of H-bond interaction. We found good linear correlations for the dependence of some descriptors such as atomic interpenetration and hyperconjugation energy on density at bond critical point, while others like destabilization of H-atom energy, variation in N−H frequency, and NMR parameters correlate in a much worse fashion. The calculations suggest that almost all H-bonds in different base pairs belong to medium strength H-bonds. We found in thymine the H-bond interaction is more likely through the amide-type oxygen while the situation is reverse for uracil in which the urea-type oxygen is more accessible to form an H-bond. Cytosine and guanine can also form H-bonds via their amine-type or amide-type nitrogens. In cytosine, the amine-type nitrogen is involved in an N−H---O bond interaction, while, in guanine, the amide-type nitrogen has a greater contribution to H-bond interaction.

1. Introduction

The study of the hydrogen bond has long been a topic of intensive scientific research due to its significance in material science, organic and inorganic chemistry, biochemistry, and molecular medicine.[1−7] Despite the fact that hydrogen bonding is a rather old and well-known concept, still much research has been carried out to detect and define the hydrogen bond properly. However, the electronic nature of the hydrogen bond has received much attention since its discovery. Lewis originally attributed the hydrogen bond to a "secondary valence" of hydrogen.[8] Pauling argued that there are three atoms forming the hydrogen bond, the donor, the acceptor, and the hydrogen atom which is attracted by rather strong forces to two atoms.[9] However, according to Pauling's definition, the hydrogen bond is largely ionic in nature and limited to a few atoms with high electronegativities. This definition has been later developed to give detailed characteristics of the hydrogen bond.[10] A common problem of all definition is that they require terminology like partial charge and electronegativity, concepts that are not properly defined from the quantum chemistry point of view. Another definition was given by Pimentel and McClellan: "A hydrogen bond is said to exist when (1) there is an evidence of a bond and (2) the bond involves a hydrogen atom already bonded to another atom."[11] This definition is very open and does not make any assumption about the nature of donor and acceptor groups.

From a quantum chemistry point of view, there are different concepts that can be considered as useful criteria to detect and measure the hydrogen bond strength. The interaction energy of the hydrogen bond that can be obtained by subtracting the total energy of the complex from the corresponding isolated species is the first criterion reflecting the H-bond strength.[12] However, this approach is problematic and can be performed just for the intermolecular interaction. Moreover, it cannot be applied to determine individual H-bond energies if more than one H-bond presents.

However, only a few studies have been devoted to evaluate the individual H-bond strength. For DNA base pairs, Dannenberg at al. suggested that the energy of a given HB could be estimated by computing the binding energy of a hypothetical twisted structure, in which two bases are bonded by this HB only.[13] This strategy is expected to be useful in many cases but not generally applicable for complexes with complicated structures because it may be difficult to form a hypothetical structure with only one H-bond but without causing other steric interactions. Grunenberg suggested that compliance constants could be employed as unique bond strength descriptors.[14] Although, this approach has been criticized by Baker and Pulay, who concluded that a compliance constant might not be suitable for describing individual bonding interactions,[15] in a very recent study Grunenberg showed that the numerical stability of compliance constants makes them indeed valid bond descriptors for both covalent bonds and noncovalent interactions such as hydrogen bonding.[16] Li and co-workers proposed a simple atom replacement approach for estimating the individual contribution of each H bond in multiple hydrogen-bonded system of nucleic acid base pairs.[17]

In this study, different quantum chemical tools have been employed for testing the existence and the strength of H-bonding between nucleic acid bases. Among nucleic acid base pairs, the well-known Watson−Crick (W−C) guanine−cytosine and adenine−thymine pairs involve three and two normal hydrogen bonds, respectively.[18] They belong to medium strength hydrogen bonds, often having double wells on the corresponding proton-transfer potential energy surface.[19] Besides these regular W−C interactions, a large array of possible base pair interactions involving two hydrogen bonds have been enumerated and many of them have been observed in crystal structure.[20] Theoretical

* Corresponding author. E-mail: mohajeri@susc.ac.ir.

10.1021/jp075992a CCC: $40.75
Published on Web 12/18/2007

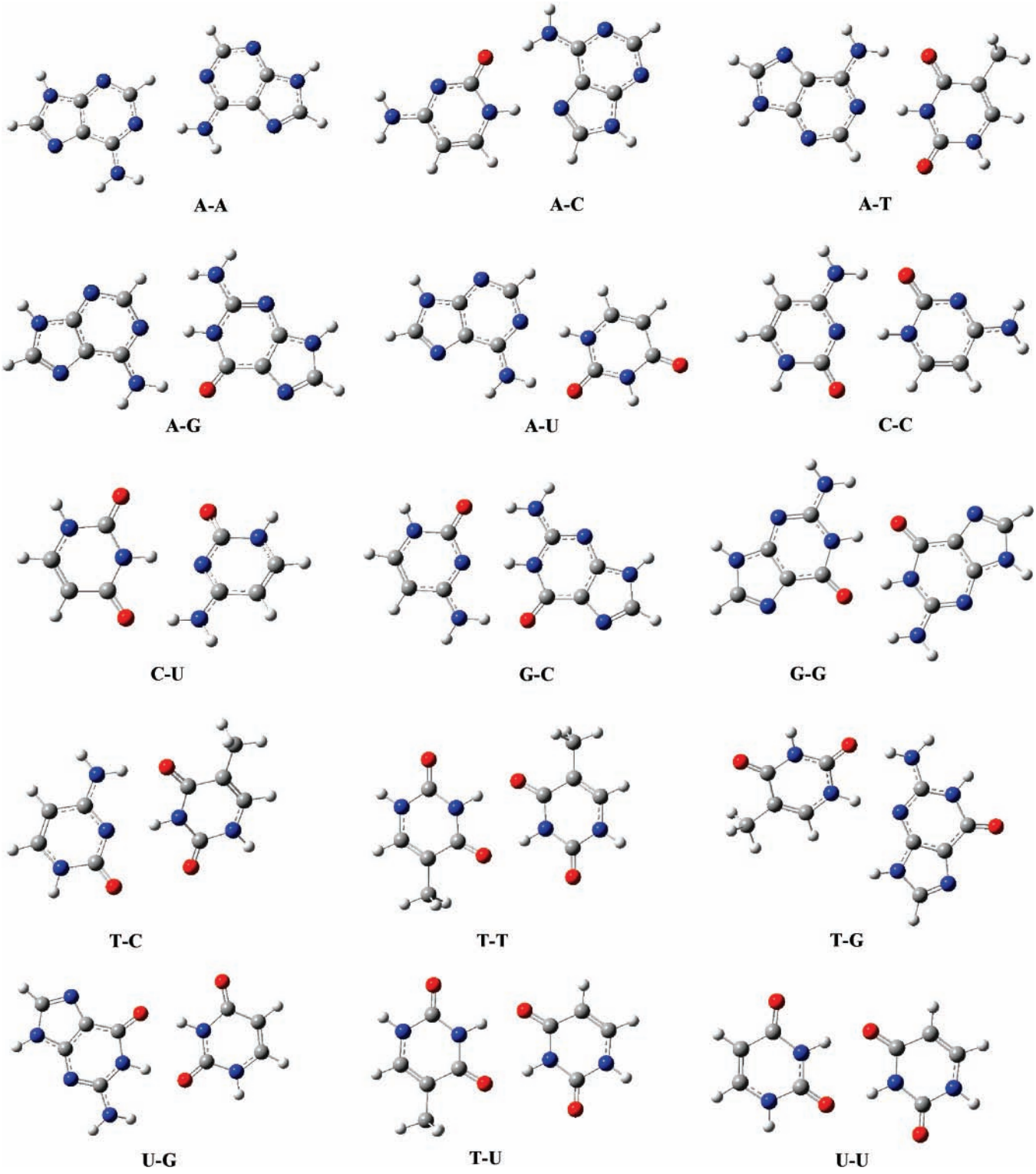

Figure 1. Optimized structures of H-bonded nucleic acid base pairs.

investigations were intensely applied to study nucleic acid base pairs and their H-bonded and stacked complexes.[21−24] Most of ab initio studies of nucleic acid bases focused on the optimization of geometries of base pairs and calculation of total interaction energies at the minima. Nevertheless, the evaluation of individual strength of each H-bond is also important for design of new strategies for molecular recognition or supramolecular assemblies.

In this research, we wish to find deep insight into the nature of the H-bond interaction in nucleic acid base pairs by applying different quantum chemical tools. Our main objectives are first to provide an ultimate picture of the origin and then to find reliable criteria for evaluation of H-bond strength.

2. Computational Details

The calculations carried out in this research have been done with the Gaussian 03 program.[25] Becke's three-parameter exchange functional with LYP correlation functional (B3LYP) and basis set 6-31+G* were used. This method was applied to

TABLE 1: Bond Length (Å), Frequency (cm^{-1}), % s Character, Population of σ^*, Density, Laplacian of Electron Density (au) of N−H Bonds, and Hydrogen Atom Energy (au) for Isolated Nucleic Acid Bases Calculated at B3LYP/6-31+G* [a]

NAB	ν	r	% s	n_{σ^*N-H}	$\rho(r)$	$\nabla^2\rho(r)$	E_H
adenine							
N4−H	3604	1.00 95	30.71	0.010 04	0.3038	0.3690	−0.404
uracil							
N1−H	3631	1.01 17	29.09	0.012 96	0.3299	0.4199	−0.425
N3−H	3592	1.01 54	28.75	0.015 33	0.3264	0.4147	−0.419
cytosine							
N1−H	3612	1.01 27	29.06	0.015 61	0.3299	0.4188	−0.432
N4−H	3603	1.01 06	30.49	0.010 49	0.3282	0.4148	−0.426
guanine							
N2−H	3599	1.00 74	31.39	0.005 93	0.2915	0.3202	−0.373
N3−H	3632	1.01 47	28.47	0.017 11	0.2109	0.1431	−0.257
thymine							
N1−H	3633	1.01 16	29.05	0.012 89	0.2320	0.1782	−0.292
N3−H	3593	1.01 52	28.65	0.015 48	0.3076	0.3533	−0.391

[a] The numbers are referred to Scheme 1.

SCHEME 1

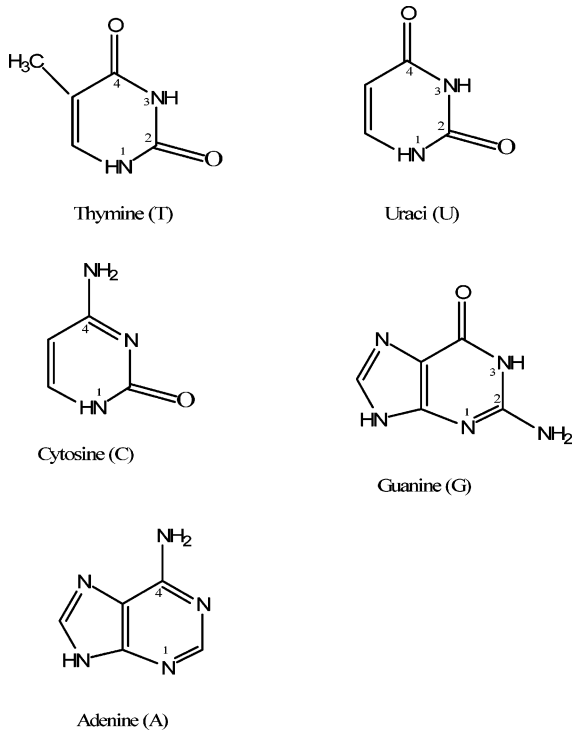

study energies, geometries, and wave functions as well as harmonic vibrational frequencies for all isolated species and complexes in Figure 1. Calculations of vibrational frequencies were performed to confirm the optimized structures are in their minima and identify frequency shifts caused by H-bond formation.

The interaction energies of base pairs were evaluated by using supramolecular method as the difference between the energy of a complex and energies of the isolated subsystems forming the complex. The calculated interaction energies were corrected for basis set superposition errors (BSSE), which were computed for all complexes using the counterpoise correction method of Boys and Bernardi.[26]

The obtained wave functions were used for the topological analyses of the electron densities. The AIM2000 program was employed for calculating the bond critical points and visualizing the bond paths.[27] The natural bond orbital (NBO) analysis has been also employed to evaluate the charge-transfer process during the complex formation.[28] The gauge-induced atomic orbital (GIAO) approach was used to calculate the NMR properties.[29]

TABLE 2: Interaction Energies with BSSE Correction (kcal/mol) of Base Pairs and the Total Energies of Their Isolated Fragments (au)

X−Y	E_X	E_Y	E_{XY}	ΔE
G−C	−542.5754	−394.9497	−937.5677	−26.73
G−G	−542.5754	−542.5754	−1085.1904	−24.85
C−C	−394.9497	−394.9497	−789.9325	−21.08
U−G	−414.8376	−542.5754	−957.4366	−14.81
A−G	−467.3398	−542.5754	−1009.9382	−14.42
A−U	−467.3398	−414.8376	−882.1987	−13.37
A−T	−467.3398	−454.1559	−921.5179	−13.14
T−G	−454.1559	−542.5754	−996.7521	−13.09
A−C	−467.3398	−394.9497	−862.3102	−13.02
T−T	−454.1559	−454.1559	−908.3338	−12.93
T−U	−454.1559	−414.8376	−869.0121	−11.61
T−C	−454.1559	−394.9497	−849.1255	−11.52
C−U	−394.9497	−414.8376	−809.8056	−10.52
U−U	−414.8376	−414.8376	−829.6909	−9.88
A−A	−467.3398	−467.3398	−934.6880	−4.71

3. Results and Discussion

In this work, a variety of hydrogen bonds between different nucleic acid bases (NAB) has been theoretically studied using density functional calculation. Five bases are considered, adenine (A), cytosine (C), uracil (U), guanine (G), and thymine (T) (Scheme 1). The structural parameters of NABs are given in Table 1. The detection of H-bonds and evaluation of their strengths for 15 H-bonded complexes of five nucleic acid bases have been studied using (1) geometrical and energetic criteria, (2) atoms in molecules topological parameters, (3) NBO analysis, and (4) spectroscopic measurements, which are discussed in the following sections.

3.1. Geometrical and Energetic Criteria. Traditionally, the interaction energy due to H-bond formation has been used to categorize this interaction. However, interaction energy may be applied as useful criteria where we have one H-bond. For the systems investigated here, where several H-bonds are established at the same time between the two monomers, evaluation of the H-bond strength becomes more complicated because secondary interaction may appear. Therefore, the interaction energy itself cannot be used as a reliable criteria for determination of the H-bond strength.

The interaction energies of the H-bonded base pairs as well as the energies of isolated subsystems are summarized in Table 2. The obtained values of interaction energies (ΔE) range from −4.71 to −26.73 kcal/mol. Among all base pairs, G−C with three normal H-bonds is the most stable base pair. The least interaction energy is related to A−A with one classic N---N bond and one improper C−H---N bond. Thus, the stabilization

TABLE 3: Hydrogen Bond Distance (D) and Atom···BCP Distances (d_Y, d_H) in Å, Electron Densities ($\rho(r)$), Laplacian ($\nabla^2\rho$), Kinetic Energy Density ($G(r)$), Electronic Potential Energy Density ($V(r)$), and Hydrogen Atom Energy (E_H) in au

pairs	D	d_Y	d_H	$\rho(r)$	$\nabla^2\rho(r)$	$G(r)$	$V(r)$	E_H
A−C								
NH---N	1.9591	2.4066	1.2956	0.029 86	0.083 16	0.021 42	0.022 06	−0.393
NH---O	1.8369	2.2337	1.2395	0.032 15	0.107 72	0.027 04	0.027 16	−0.389
A−U								
NH---N	1.9023	2.3609	1.2340	0.034 74	0.091 60	0.024 28	0.025 66	−0.385
NH---O	1.8978	2.2963	1.2927	0.028 72	0.092 24	0.023 54	0.024 02	−0.396
A−T								
NH---N	1.8700	2.3299	1.2041	0.036 92	0.098 08	0.026 03	0.027 55	−0.380
NH---O	1.9272	2.3250	1.3200	0.026 99	0.085 92	0.021 97	0.022 45	−0.391
CH---O	2.9359	3.2754	2.2824	0.003 70	0.014 45	0.002 76	0.001 91	−0.582
A−A								
NH---N	2.0752	2.5187	1.4045	0.023 15	0.066 16	0.016 65	0.016 76	−0.569
CH---N	2.5613	2.9621	1.8786	0.009 74	0.029 32	0.006 47	0.005 60	−0.402
A−G								
NH---N	1.9586	2.4122	1.2893	0.030 95	0.082 20	0.021 61	0.022 66	−0.393
NH---O	1.8486	2.2534	1.2424	0.032 37	0.102 84	0.026 34	0.026 98	−0.389
C−C								
NH---N	1.8592	2.3120	1.2016	0.037 32	0.102 88	0.027 09	0.028 47	−0.386
NH---O	1.8031	2.2154	1.1945	0.035 84	0.113 28	0.029 03	0.029 74	−0.378
G−C								
NH---N	1.9354	2.3831	1.2745	0.031 78	0.088 48	0.022 98	0.023 83	−0.399
NH---O	1.7884	2.2014	1.1806	0.036 95	0.117 44	0.030 04	0.030 72	−0.378
NH---O	1.9192	2.3196	1.3091	0.027 69	0.087 08	0.022 38	0.022 99	−0.395
T−C								
NH---N	2.0020	2.4552	1.3288	0.027 11	0.074 80	0.019 17	0.019 63	−0.383
NH---O	1.8577	2.2586	1.2543	0.031 50	0.101 32	0.025 85	0.026 36	−0.392
C−U								
NH---N	1.9952	2.4489	1.3223	0.027 54	0.075 76	0.019 45	0.019 95	−0.382
NH---O	1.8557	2.2566	1.2526	0.031 62	0.101 84	0.025 96	0.026 46	−0.392
G−G								
NH---O	1.7648	2.1784	1.1573	0.041 01	0.125 62	0.032 92	0.034 36	−0.394
NH---O	1.7647	2.1778	1.1572	0.041 01	0.125 62	0.032 92	0.034 37	−0.393
T−G								
NH---N	1.9530	2.4022	1.2885	0.030 55	0.083 12	0.021 65	0.022 50	−0.391
NH---O	1.7884	2.2705	1.2638	0.027 69	0.087 08	0.022 38	0.022 99	−0.393
T−U								
NO---O	1.8542	2.2558	1.2519	0.031 05	0.101 36	0.025 59	0.025 84	−0.384
NH---O	1.8652	2.2658	1.2628	0.030 28	0.098 72	0.024 94	0.025 19	−0.386
T−T								
NH---O	1.8607	2.2618	1.2583	0.030 60	0.099 80	0.025 21	0.025 47	−0.385
NH---O	1.8610	2.2620	1.2585	0.030 59	0.099 76	0.025 20	0.025 46	−0.385
U−G								
NH---O	1.8243	2.2241	1.2248	0.034 34	0.111 16	0.028 40	0.029 01	−0.378
NH---O	1.8409	2.2496	1.2331	0.032 51	0.102 40	0.026 17	0.026 73	−0.401
U−U								
NH---O	1.8766	2.2736	1.2764	0.029 25	0.096 56	0.024 30	0.024 45	−0.386
NH---O	1.8772	2.2751	1.2769	0.029 33	0.096 16	0.024 22	0.024 40	−0.387

caused due to H-bond formation in an improper C−H---N bond is less significant and almost negligible compared to the classic N−H---N bond. There is also an interaction between hydrogen of the C−H group and oxygen of the carbonyl group in the A−T base pair, leading to formation of a C−H---O═C hydrogen bond. Recently, theoretical and experimental investigations on the weak C−H---O and C−H---N interactions have received attention due their occurrence in proteins, amino acids, and nucleic acid base pairs.[30−32]

In addition to the interaction energy, the geometry of the complexes, especially the H-bond distance and the X−H---Y angle, will provide another indication of directionality of the interaction and is an essential characteristic of the H-bond. The structures of the base pairs without geometrical constraints are presented in Figure 1. The H-bond distances and the X−H---Y angles are reported in Tables 3 and 4, respectively. It is apparent that all H-bonds are almost linear. The greatest deviations from linearity, 48.1 and 32.8°, are related to the case of weak C−H---O and C−H--N hydrogen bonding in A−T and A−A base pairs, respectively.

The structures in Figure 1 show that some base pairs are nonplanar. One of the most prominent sources of nonplanarity of pairs is the pyramidalization of the amino groups of the bases. Nonplanarity is apparent for T−G, A−G, and T−C base pairs. The pyramidalization of guanine is more significant compared to that of adenine and cytosine.[33] Further, pyramidalization of the guanine amino group is highly asymmetrical due to the repulsion between the hydrogen of NH and the adjacent amino group hydrogen atom. Also, asymmetry is observed for the cytosine amino group due to the repulsion with adjacent CH. However, the amino group hydrogens can participate in out-of-plane H-bonds where the hydrogens are bent away from the molecular plane of base. In other pairs the amino group is planarized as a result of H-bond formation.

3.2. Atoms in Molecules Topological Parameters. The theory of "atoms in molecules" (AIM) takes advantage of the electron density as an information source and can be applied to enhance our chemical insight through calculated wave functions. The theory of AIM pioneered by Bader is one of the concepts that can be used as another tool for both H-bond detection and an estimation of its strength.[34] On the basis of AIM theory, Koch and Popelier developed a series of criteria for a correct definition of an H-bond.[35] More recently, other indications such as electronic energy densities have been preferred.[36] In this work,

TABLE 4: NBO Analysis of the H-Bonded Base Pairs, Hyperconjugation Energy (kcal/mol), Frequency (cm^{-1}), Bond Distance (Å), and X−H---Y Angle (deg)

pairs	q_X	q_H	q_Y	n_{σ^*X-H}	% s	$E_n \rightarrow \sigma^*$	ν_X-H	X−H	X−H---Y
A−C									
NH---N	−0.6309	0.4727	−0.5287	0.0575	31.65	19.73	3267.58	1.0320	176.11
NH---O	−0.8080	0.4631	−0.6829	0.0445	33.93	11.47	3374.89	1.0256	167.71
A−U									
NH---N	−0.6487	0.4733	−0.6086	0.0697	31.90	24.10	3127.28	1.0394	178.53
NH---O	−0.8117	0.4571	−0.6753	0.0407	33.24	10.34	3409.05	1.0235	175.69
A−T									
NH---N	−0.6795	0.4733	−0.6006	0.0758	31.50	26.37	3060.93	1.0444	178.56
NH---O	−0.8178	0.4563	−0.6523	0.0388	33.09	9.11	3420.98	1.0228	174.12
CH---O	0.2561	0.2391	−0.6375	0.0240	32.26	0.46	3205.97	1.0874	131.90
A−A									
NH---N	−0.8261	0.4476	−0.5926	0.0395	33.06	12.24	3408.80	1.0220	175.92
CH---N	0.2524	0.2486	−0.5669	0.0290	32.14	2.61	3208.06	1.0873	147.21
A−G									
NH---N	−0.6592	0.4621	−0.6082	0.0658	30.90	20.73	3185.23	1.0369	179.35
NH---O	−0.8105	0.4588	−0.6509	0.0493	33.06	12.36	3334.32	1.0279	177.17
C−C									
NH---N	−0.6245	0.4702	−0.6498	0.0722	31.96	25.60	3154.74	1.0373	176.99
NH---O	−0.8033	0.4695	−0.6986	0.0565	33.59	16.47	3226.87	1.0356	177.66
G−C									
NH---N	−0.6576	0.4601	−0.6450	0.0632	30.91	20.80	3253.23	1.0327	177.15
NH---O	−0.8485	0.4574	−0.6870	0.0589	33.92	16.60	3404.03	1.0364	178.72
NH---O	−0.7966	0.4692	−0.6782	0.0383	33.62	10.41	3192.84	1.0238	178.08
T−C									
NH---N	−0.6755	0.4799	−0.6415	0.0577	31.29	16.70	3209.54	1.0373	169.65
NH---O	−0.8181	0.4598	−0.6597	0.0463	32.50	10.89	3361.36	1.0267	175.23
C−U									
NH---N	−0.6787	0.4803	−0.6539	0.0774	32.14	26.78	3005.53	1.0379	169.41
NH---O	−0.8129	0.4625	−0.6690	0.0542	33.44	15.69	3303.18	1.0266	175.31
G−G									
NH---O	−0.6536	0.4611	−0.689	0.0740	30.97	21.67	3186.08	1.0375	172.90
NH---O	−0.6536	0.4611	−0.689	0.0740	30.98	21.68	3186.08	1.0375	172.89
T−G									
NH---N	−0.6457	0.4698	−0.6357	0.0613	31.57	19.75	3232.25	1.0335	175.62
NH---O	−0.8482	0.4617	−0.6787	0.0431	32.10	11.15	3366.14	1.0264	175.53
T−U									
NH---O	−0.6825	0.4840	−0.6513	0.0526	31.10	10.76	3316.76	1.0329	170.75
NH---O	−0.6758	0.4833	−0.6426	0.0517	30.99	11.10	3316.76	1.0323	170.66
T−T									
NH---O	−0.6763	0.4835	−0.6499	0.0520	31.00	10.87	3285.77	1.0325	170.88
NH---O	−0.6763	0.4835	−0.6499	0.0520	31.00	10.86	3285.77	1.0325	170.92
U−G									
NH---O	−0.6807	0.4868	−0.6501	0.0587	31.43	14.16	3322.98	1.0293	176.64
NH---O	−0.6575	0.4638	−0.6999	0.0570	30.70	13.43	3201.54	1.0384	172.56
U−U									
NH---O	−0.6828	0.4838	−0.6726	0.0484	30.94	9.72	3344.46	1.0307	169.92
NH---O	−0.6834	0.4839	−0.6424	0.0496	31.04	9.75	3344.46	1.0315	168.68

the wave functions of H-bonded complexes obtained at the B3LYP/6-31+G* level have been used to characterize topological properties of the electronic charge density. The following characteristics of bond critical points (BCPs) are taken into account: density at BCP; its Laplacian; the electronic kinetic energy density $G(r)$; the electronic potential energy density $V(r)$. The results of AIM topological parameters for individual H-bonds in each complex are listed in Table 3. According to the AIM point of view, the detection of a hydrogen bond and evaluation of its strength can be demonstrated by the following criteria:

Electron Density of the Bond Critical Point. According to Bader theory, identification of the critical point (CP) and the existence of a bond path in equilibrium geometry are both necessary and sufficient conditions for the presence of a bond between two atoms.[37] On the other hand, Cioslowski and coworkers have claimed that the existence of a bond path between a pair of nuclei is not necessarily indicative of an attractive bonding interaction between them. Instead it should be interpreted as either bonding or nonbonding or attractive or repulsive interactions.[38] The results of recent studies carried out by Bickelhaupt et al. confirm that the presence of a bond critical point and bond path can only show the contact between charge distribution and can be stabilizing or destabilizing.[39] Therefore, interpretation of the AIM topological parameters should be carried out with care.

However, in medium strength hydrogen bonds the values of density at the BCP are relatively low and do fall within the range 0.002−0.04 au. In Table 3 we see that the densities at BCP for all of the H-bonds in different base pairs fall within the above-mentioned typical range. The least values, 0.0097 and 0.0033 au, are related to the case of weak C−H---N and C−H---O hydrogen bondings in A−A and A−T base pairs, respectively. Figures 2 and 3 present the correlation between density at the BCP and H-bond distance for N---H and O---H bonds. The linear correlation coefficients are calculated to be 0.980 and 0.965 for N−H---N and N−H---O bonds, respectively.

In general, the results demonstrate that the case where two monomers interact in a direction in which Y locates in line with X−H, i.e., in the case of linear X−H---Y, the H-bond interaction becomes stronger and the density at the BCP of H---Y increases.

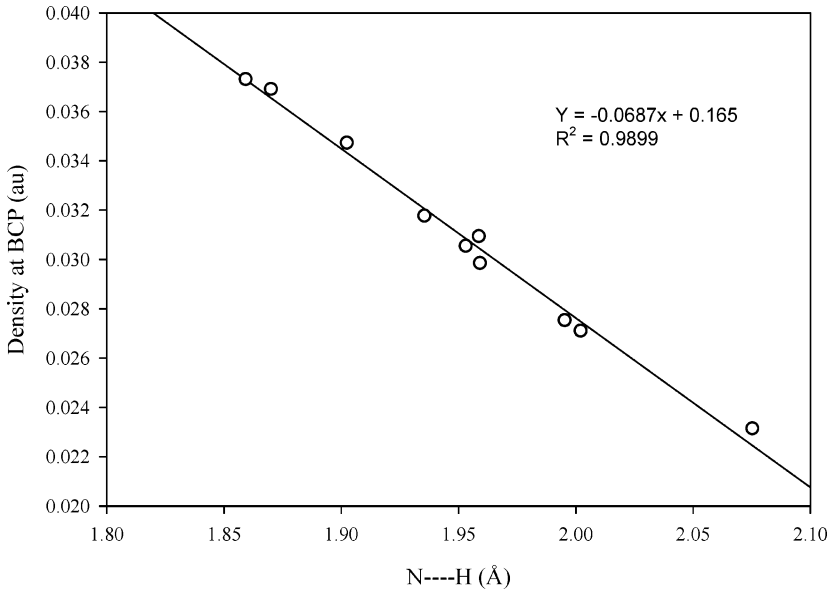

Figure 2. Relation between the density at BCP and the N---H distance.

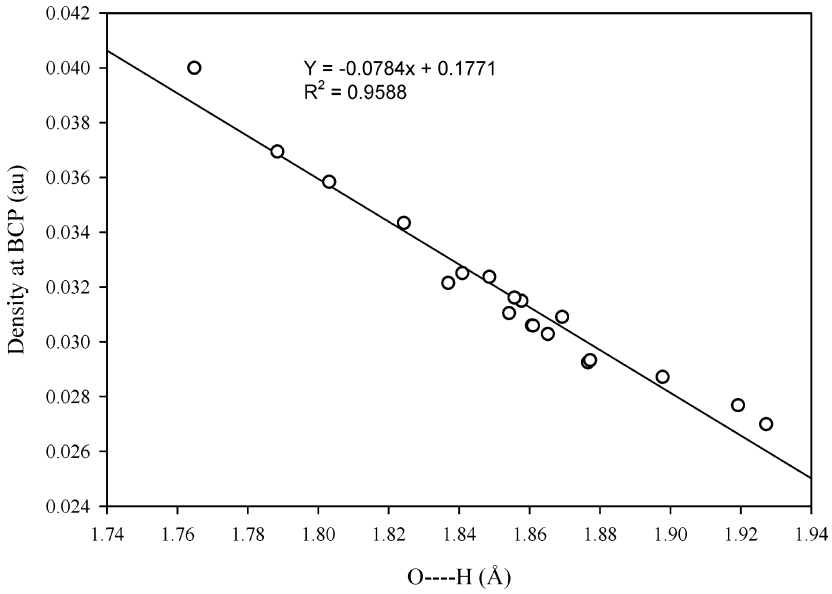

Figure 3. Relation between the density at BCP and the O---H distance.

Electronic Energies Density. Bonds can be further characterized by evaluating of Laplacian of electron density which is related to the bond interaction energy by a local expression of the virial theorem[34]

$$\left(\frac{\hbar^2}{4m}\right)\nabla^2\rho(r) = 2G(r) + V(r) \qquad (1)$$

where $G(r)$ is the electronic kinetic energy density, which is always positive. $V(r)$ is the electronic potential energy density and must be negative.[40] The sign and the value of $\nabla^2\rho(r)$ at the bond critical point characterize the bond nature. A negative $\nabla^2\rho(r)$ shows the excess potential energy at BCP introducing electronic charge concentration in the internuclear region and implies a shared interaction as in covalent bonds. A positive value for $\nabla^2\rho(r)$, in contrast, shows the greater contribution of kinetic energy and shows the positive curvature of $\rho(r)$ along the interaction line, as the Pauli exclusion principle leads to a relative depletion of charge density in the interatomic surface. Thus, the interaction is dominated by the contraction of charge density away from interatomic surface toward each of the interaction species (closed-shell interaction).

The electronic energy density $H(r)$ at BCP is given by[41]

$$H(r) = G(r) + V(r) \qquad (2)$$

In the normal H-bond both $\nabla^2\rho(r)$ and $H(r)$ at BCP are positive. The condition in which $|V(r)| < 2G(r)$ and $|V(r)| > G(r)$ provides a positive value for $\nabla^2\rho(r)$ leading to a closed-shell interaction, while $H(r)$ is negative and shows a shared interaction. This type of interaction is characterized to be partially covalent and partially electrostatic.[42]

The results in Table 3 show the positive values for the Laplacian of electron density in all cases. In addition, $|V(r)| \approx G(r)$ causes a near to zero value for $H(r)$ leading to a medium strength H-bond with closed-shell character. Figures 4 and 5 present energetic properties of BCP for N−H---N and N−H---O bonds, respectively. It is apparent that both $G(r)$ and $V(r)$ are well correlated to H-bond distance.

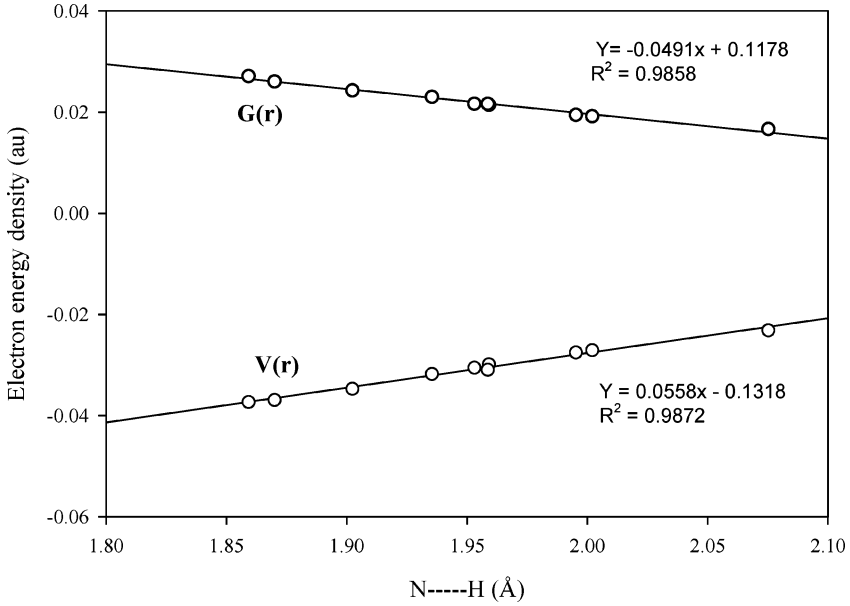

Figure 4. Relationship between the energy properties ($G(r)$ and $V(r)$) of BCP and the N---H distance.

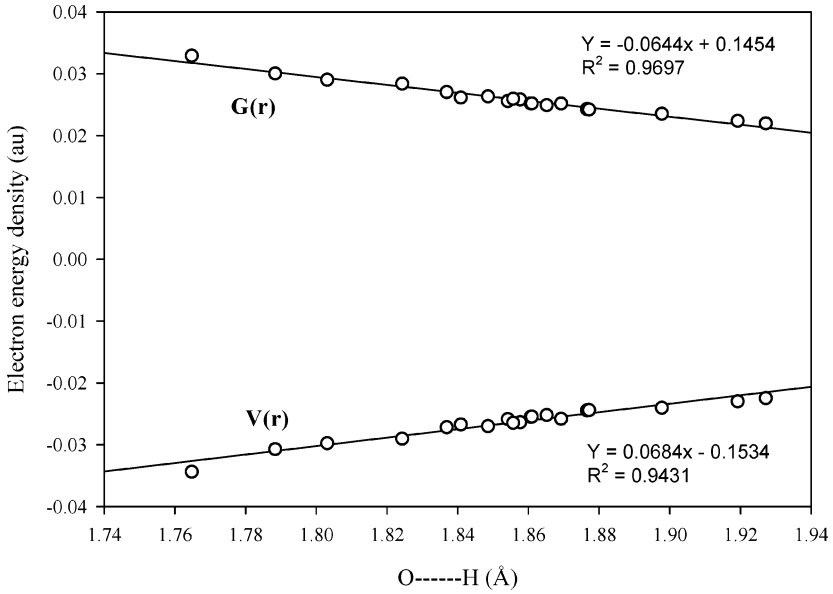

Figure 5. Relationship between the energy properties ($G(r)$ and $V(r)$) of BCP and the O---H distance.

The extent of the validity of Abramov's expression has been also investigated for the base pairs investigated here to obtain kinetic energy density at BCP,[43]

$$G(r) = 3/10(3\pi^2)^{2/3}\rho^{5/3}(r) + (1/6)\nabla^2\rho(r) \qquad (3)$$

The percents of deviation between the calculated $G(r)$ from eq 3 and the obtained values by use of AIM theory range from 0.04% to 4.4% in different base pairs.

Atomic Interpenetration. A hydrogen bond results from the mutual penetration of the van der Waals envelopes of the H atom and of the atom Y. The nonbonded radius of an atom Y (r_o(Y)) is defined as the distance of its nucleus to a given electron density contour in its isolated fragment. Usually a value of 0.001 au for the contour is taken because this yields molecular sizes and atomic diameters in good agreement with gas-phase van der Waals radii. The bonded radius [r_b(Y)] is then simply the distance from the nucleus to the BCP of the H---Y in the hydrogen-bonded complex. The penetration Δr(Y) is defined as the nonbonded radius minus the bonded radius. This is a concept unique to AIM which represents an assumption of atomic interpenetration and determines whether hydrogen bonding is likely between donor and acceptor. Further, the strength of the interaction increases with the degree of atomic interpenetration.

In this study, the van der Waals atomic radii have been used as nonbonded atomic radii, which are given by Pauling.[10] Thus the atomic interpenetration can be defined as Δr(Y) + Δr(H). The correlations between density at BCP and atomic interpenetration are presented in Figures 6 and 7 for N−H---N and N−H---O bonds, respectively. The results demonstrate penetration between 0.5 and 0.85 au for H---N bonds, while the calculated penetrations are larger for H---O bonds (Figure 7).

Energetic Destabilization of the Hydrogen Atom. This criterion requires that the hydrogen atom involved in H-bond formation be destabilized upon complex formation; that is, its energy should rise.[44] The extent of destabilization can be calculated as the difference between E_H for the involved hydrogen in the base pair (Table 3) and its corresponding value in the isolated base (Table 1). In all cases the H atom destabilizes

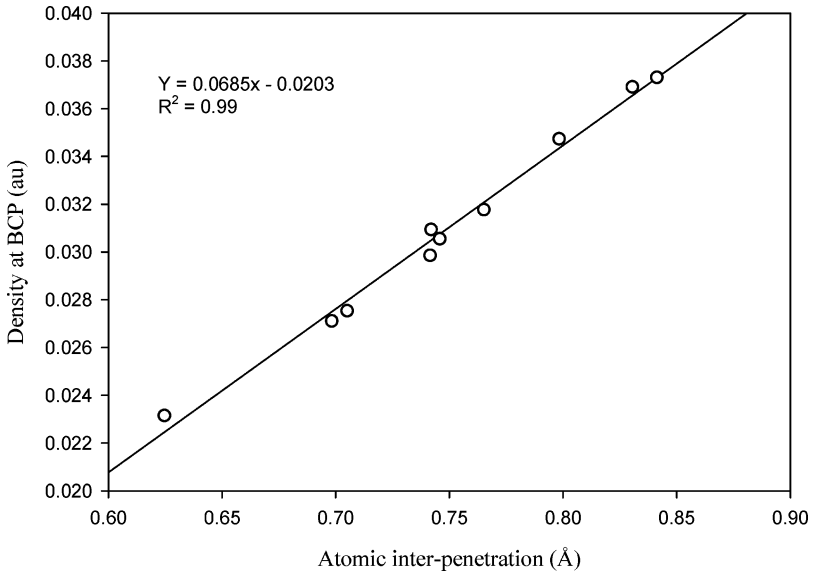

Figure 6. Correlation between density at the N---H bond critical point and atomic interpenetration.

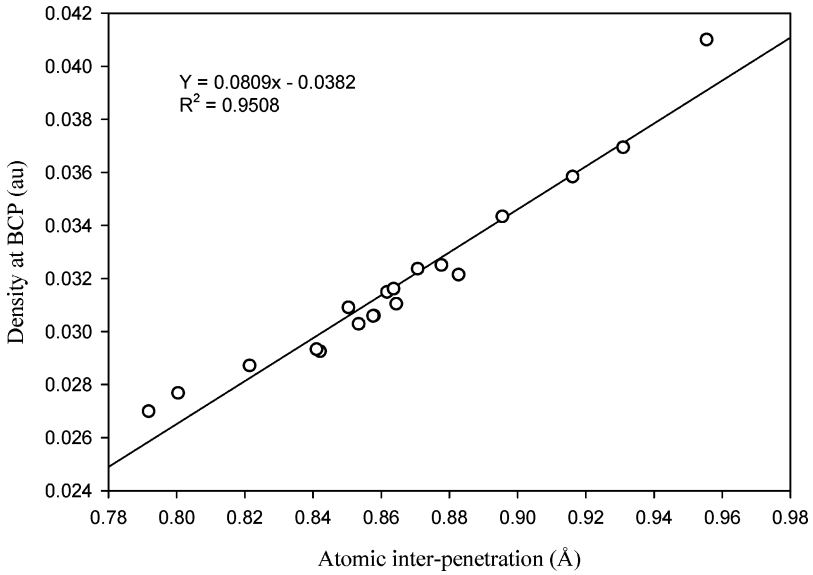

Figure 7. Correlation between density at the O---H bond critical point and atomic interpenetration.

as a result of H-bond formation. Although hydrogen atom destabilizations can be used an indicator for the presence of an H-bond in different base pairs, they do not correlate well with density at BCP. Thus, this criterion cannot be considered as a general and reliable tool for evaluation of H-bond strength.

3.3. Natural Bond Orbital Analysis. A characteristic feature of X−H---Y formation is X−H bond weakening. This weakening is accompanied by bond elongation and thus decreases the X−H stretching vibrational frequency in comparison to the noninteracting species. This shift to lower frequency in normal H-bonds, which is called red shift, represents one of the important manifestation of the H-bond formation.[45]

AIM analysis does not reveal the origin of the red-shifted H-bonds. This problem can be solved by performing a natural bond orbital calculation. The natural bond orbital (NBO) analysis transforms the canonical delocalized Hartree−Fock molecular orbitals into localized orbitals that are closely tied to chemical bonding concepts. NBO stresses the role of intermolecular orbital interaction in the complex, which can be used as a measure for electron delocalization. The results of NBO analysis for all base pairs are collected in Table 4.

Alabugin et al. showed that the X−H bond length in the X−H---Y hydrogen-bonded complex is controlled by a balance of two main factors acting in opposite directions.[46] The first is the hyperconjugative interaction (charge transfer) from the lone pair of Y to an antibonding σ^* orbital of X−H leading to an increase in population of antibonding orbital weakens and elongates the X−H bond. Hyperconjugation energy, $E_{n\rightarrow\sigma^*} = -q\langle n|F|\sigma^*\rangle^2/\epsilon_{\sigma^*} - \epsilon_n$, is the second-order perturbation energy of interaction between donor NBO, which is the lone pair of Y, and an acceptor NBO σ^* of X−H.

The importance of charge transfer is well documented by Weinhold and co-workers, who have shown that, in the absence of this donor−acceptor orbital interaction, electrostatic and other interactions cannot lead to a characteristic close approach and strong interaction of H-bonded species.[28,47] Nevertheless, in a more recent study, Bickelhaupt et al. confirmed and quantified that the charge transfers caused by donor−acceptor interactions are the same order of magnitude as the electrostatic term.[48]

Therefore, the amount of hyperconjugation energy can be used as another criterion for determination of the H-bond strength. The relationships between $E_{n\rightarrow\sigma^*}$ and the density at

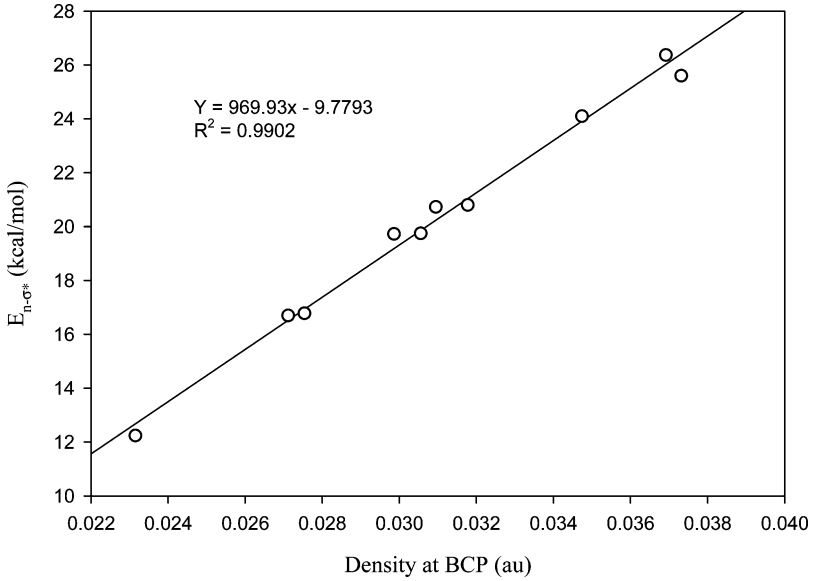

Figure 8. Correlation between hyperconjugation energy and density at BCP for N---H bonds.

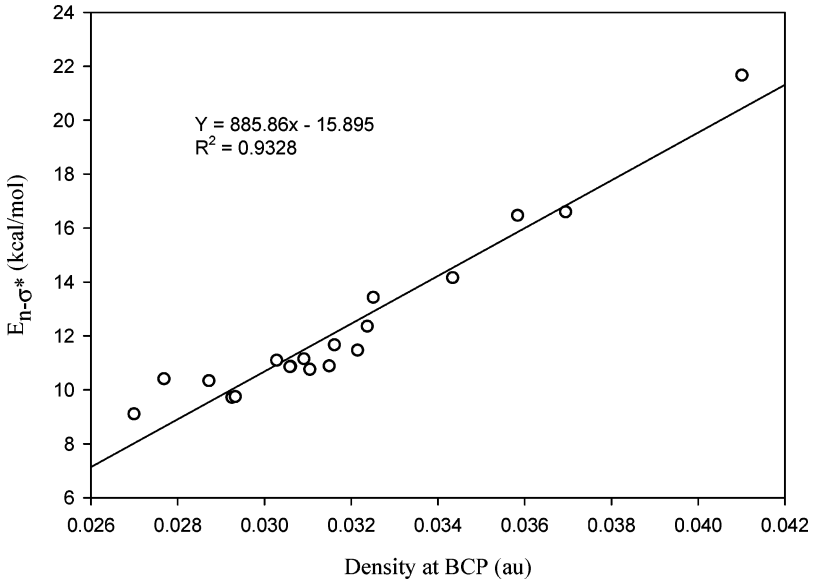

Figure 9. Correlation between hyperconjugation energy and density at BCP for O---H bonds.

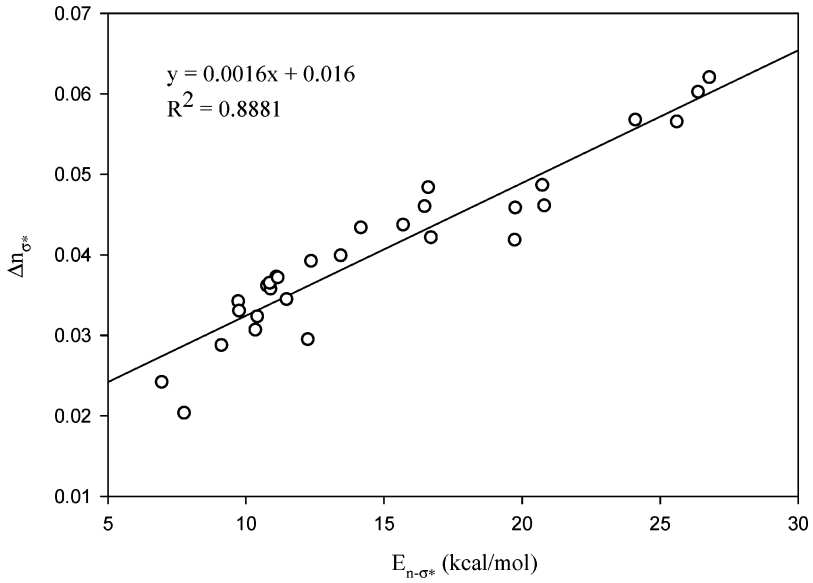

Figure 10. Relationship between Δn_{σ^*} and hyperconjugation energy.

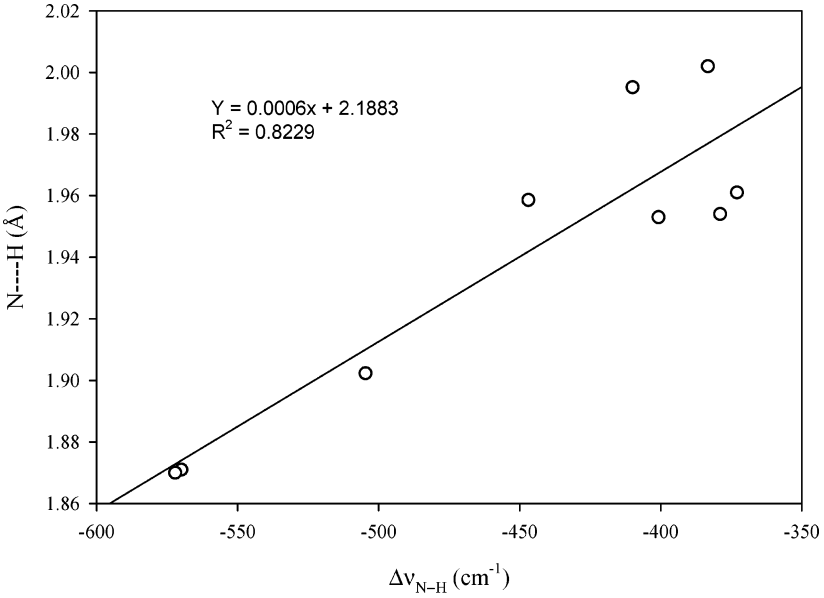

Figure 11. Correlation between N---H distances and $\Delta\nu_{N-H}$.

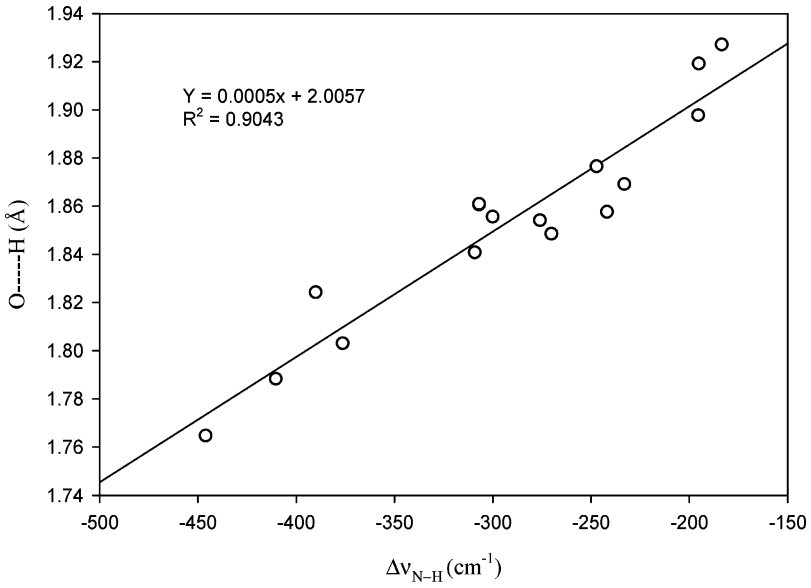

Figure 12. Correlation between O---H distances and $\Delta\nu_{N-H}$.

BCP are illustrated in Figures 8 and 9 for N---H and O---H bonds, respectively. In addition, the increase in population of antibonding σ^* of X−H (Δn_{σ^*}) correlates with the hyperconjugation energy (Figure 10).

The second factor is rehybridization which accompanying repolarization of the X−H bond upon H-bond formation makes hydrogen more electropositive such that the s character of the X-hybrid atomic orbital of X−H increases leading to contraction and has a shortening effect on the X−H bond. Hyperconjugation and rehybridization act in opposite directions; thus, a red or blue shift of the X−H bond is a balance of the two effects.

According to the obtained results, in all N−H---N and N−H---O hydrogen bonds the hyperconjugation is dominant, leading to the elongation and red shift for N−H bonds. Figures 11 and 12 demonstrate that the variation of the H-bond distance is linearly correlated with stretch frequency shift of the N−H bond. In contrast to normal hydrogen bonds, for the C−H---N bond in A−A and C−H---O bond in A−T, where $E_{n\rightarrow\sigma^*}$ is less than 5 kcal/mol, the molecular structure allows significant rehybridization of the C−H bond leading to the shortening and blue shift for it.

3.4. Spectroscopic Methods. In addition to structure and energetic determination, several spectroscopic techniques were used to gain information about the H-bonded complex. Among them, nuclear magnetic resonance (NMR) and nuclear quadrupole resonance (NQR) measurements have been most often employed for testing the existence and the strength of an H-bond.[49−51] It has been demonstrated that the nitrogen and oxygen chemical shifts are sensitive to the existence of an H-bond.[52,53] In this part, NMR parameters including quadrupole coupling constants and isotropic chemical shifts at oxygen and nitrogen nuclei have been reported to investigate the H-bonding effects on ^{17}O and ^{14}N tensors in more detail. To make a direct comparison between the calculated isotropic chemical shielding (σ_{iso}) and the observed chemical shift, we use the scale of 287.5 and 264.5 ppm established by Waylishen for ^{17}O and ^{14}N, respectively.[54]

TABLE 5: Calculated ^{17}O and ^{14}N NMR Tensors for Free Nucleic Acid Bases and Their Pairings[a]

species	σ_{11} (ppm)	σ_{22} ppm	σ_{33} ppm	σ_{iso} ppm	δ_{iso} ppm	C_Q MHz	η_Q
^{17}O-cytosine	−151	−98	277	9	278	8.60	0.31
A−C	−85	−69	267	37	250	8.13	0.55
C−C	−63	−59	271	50	238	7.50	0.64
G−C	−73	−46	268	50	237	7.78	0.61
^{17}O-guanine	−180	−166	330	-5	283	8.62	0.24
A−G	−160	−88	327	26	261	8.23	0.47
C−G	−139	−53	326	45	242	8.00	0.59
G−G	−105	−54	320	53	234	7.91	0.67
U−G	−124	−115	326	29	258	8.17	0.49
^{17}O-thymine	−328	−143	337	-47	334	9.13	0.13
A−T	−253	−123	327	16	303	8.74	0.31
C−T	−236	−106	308	11	298	8.70	0.34
T−T	−195	−176	320	17	304	8.74	0.32
U−T	−196	−170	306	20	307	8.76	0.32
^{17}O2-thymine	−88	−69	289	44	243	8.07	0.47
G−T	−29	−27	265	69	217	7.58	0.72
^{17}O2-uracil	−103	−75	291	38	250	8.10	0.44
A−U	−53	−40	287	64	222	7.69	0.68
G−U	−29	−17	280	78	209	7.48	0.80
U−U	−65	−27	284	64	223	7.72	0.67
^{17}O4-uracil	−297	−184	313	-56	343	9.23	0.11
C−U	−213	−125	279	20	267	8.92	0.47
U−U	−263	−105	306	21	308	8.80	0.32
^{14}N4-adenine	174	202	188	188	76	4.49	0.13
A−A	160	185	189	178	86	3.99	0.26
A−C	160	163	185	169	95	3.63	0.4
A−U	153	178	202	178	87	3.79	0.32
A−G	154	168	202	175	90	3.63	0.37
A−T	158	180	202	180	84	3.88	0.30
^{14}N1-cytosine	43	123	171	112	152	3.25	0.07
A−C	48	122	238	23	241	3.28	0.23
C−C	18	85	200	101	163	2.31	0.66
^{14}N4-cytosine	169	170	198	179	86	4.49	0.12
C−C	148	153	184	162	102	3.48	0.47
U−C	153	166	181	167	98	3.62	0.45
G−C	141	152	186	157	105	3.39	0.49
T−C	160	170	177	169	96	3.74	0.38
^{14}N4-uracil	65	145	173	128	137	3.83	0.10
A−U	50	111	193	118	147	3.06	0.56
^{14}N3-uracil	39	123	129	97	167	3.59	0.17
C−U	28	79	155	87	177	2.80	0.75
T−U	37	96	153	95	168	3.01	0.54
U−U	51	85	151	96	168	3.05	0.51
G−U	52	74	154	93	170	2.90	0.62
^{14}N2-guanine	157	172	253	194	70	5.03	0.16
C−G	174	180	202	185	79	4.30	0.34
^{14}N3-guanine	36	142	151	110	154	3.78	0.17
A−G	27	113	169	103	161	3.00	0.50
C−G	45	110	172	109	155	3.12	0.49
G−G	30	119	174	108	157	2.95	0.57
U−G	26	126	169	107	157	3.06	0.46
T−G	11	53	243	102	162	3.02	0.54
^{14}N1-thymine	67	149	171	129	135	3.85	0.09
G−T	62	123	185	123	141	3.22	0.47
^{14}N3-thymine	76	90	130	99	166	3.59	0.15
A−T	36	88	154	92	172	2.81	0.67
C−T	40	92	154	95	169	2.99	0.55
T−T	36	99	155	97	167	2.99	0.53
U−T	39	97	154	97	167	3.00	0.52

[a] Numbers are referred to Scheme 1.

The nuclear quadrupole resonance (NQR) arises from the interaction between the nuclear quadrupole moment Q and the electric field gradient (EFG) at the nucleus position. In general, the nuclear quadrupole coupling constant (C_Q) and asymmetry parameter (η_Q) can be theoretically computed and are found to be useful quantities for H-bond detection. The value of the quadrupole coupling constant (C_Q) of a nucleus with spin $I \geq 1$ depends on its scalar nuclear quadrupole moment Q and the EFG at the nucleus according to

$$C_Q\,(\mathrm{MHz}) = \frac{e^2 Q q_{zz}}{h} \qquad (4)$$

where e and h have their usual meaning and q_{zz} is the largest electric filed gradient tensor component (in au). The asymmetry parameter, which is defined as $\eta = |(q_{yy} - q_{xx})/q_{zz}|$, measures the deviation of the field gradient tensor from axial symmetry.

Among the wide range of $Q(^{17}\mathrm{O})$ and $Q(^{14}\mathrm{N})$ standard values published, we have selected the values $Q(^{17}\mathrm{O}) = 25.58$ mb and $Q(^{14}\mathrm{N}) = 20.44$ mb.[55] The NMR parameters of ^{17}O and ^{14}N nuclei for the base pairs as well as their values in the isolated nucleic acid bases are listed in Table 5.

^{17}O NMR and NQR. As shown in Scheme 1, the two oxygens of thymine, O2 and O4, are related to the urea- and amide-type

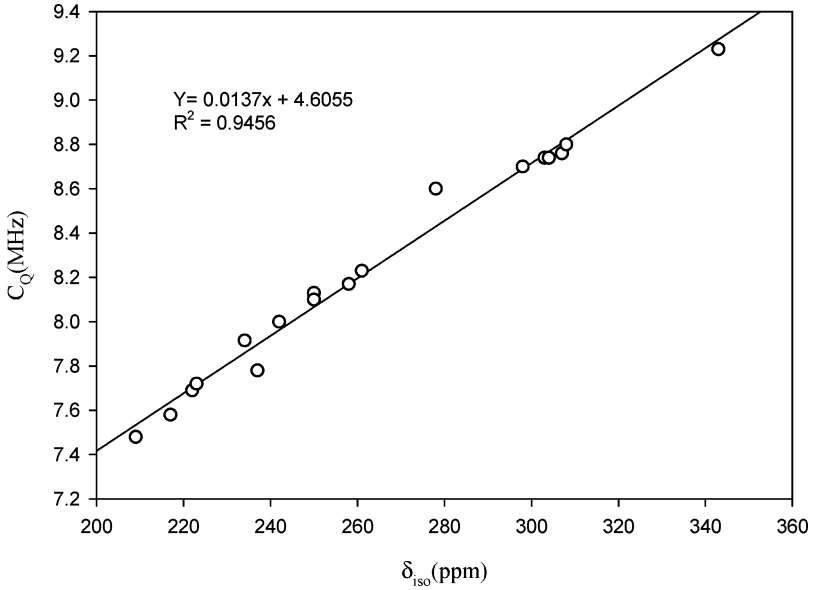

Figure 13. Correlation between the ^{17}O quadrupole coupling constants and its isotropic chemical shift.

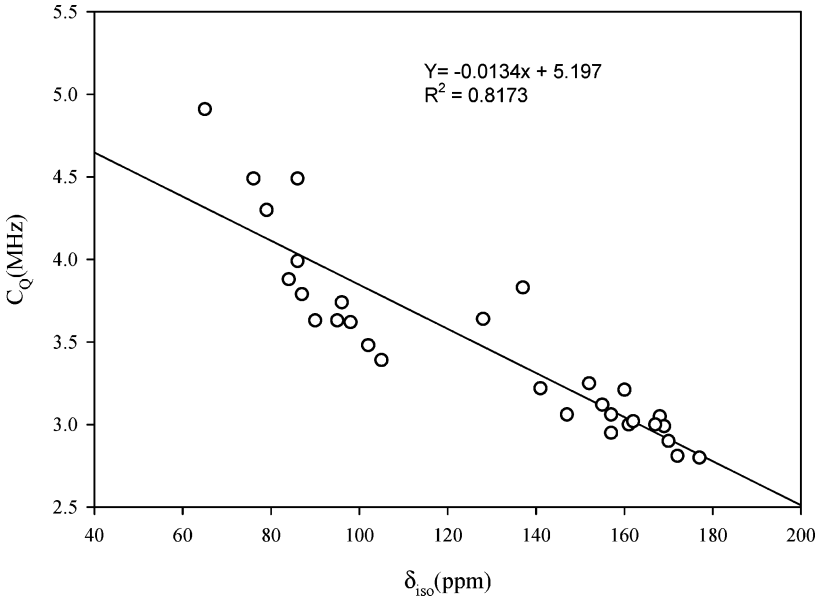

Figure 14. Correlation between the ^{14}N quadrupole coupling constants and its isotropic chemical shift.

functional groups, respectively. Consistent with its experimental result, our calculations suggest that the amide-type oxygen O4 shows much larger C_Q (9.13 MHz) than that of urea-type oxygen O2 (8.07 MHz).[56] Among five base pairs in which thymine has been involved, O4 has contributed to four of them in the C═O---H−N bond, while O2 is just involved in the G−T base pair (Table 5). This finding is in agreement with the experimental result of ^{17}O solid-state NMR study of the free nucleic acids bases reported by Wu et al.[56] that indicates O4 is free of any H-bonding interaction while O2 is responsible for a strong H-bond in the crystal packing of thymine. Therefore, O4 is more apt to be involved in H-bond formation with other nucleic acid bases. Hydrogen bond interaction at the O4 site reduces the ^{17}O quadrupole coupling constant 0.37−0.43 MHz in different base pairs, while C_Q of O2 is reduced 0.49 MHz in the G−T pair. The isotropic ^{17}O chemical shifts for O2 and O4 differ by 125 ppm. In all base pairs the chemical shift of ^{17}O nuclei moves downfield as the result of H-bond formation. Parallel to C_Q and δ_{iso}, the asymmetry parameter is also influenced by the H-bonding interaction. The amount of increase in η_Q is 0.18−0.21 and 0.25 at O4 and O2, respectively. Thus, the increase in η_Q is in line with the increase in the strength of the H-bond interaction.

In contrast to thymine, the H-bond in uracil is more likely at the O2 site. This result is in accordance with the experimental solid-state ^{17}O NMR study of uracil, which indicates O2 is free of intermolecular interactions.[56] Therefore, uracil can participate in H-bond interaction with other NABs via its urea-type oxygen, O2, while the amide-type oxygen (O4) is just involved in U−U and C−U base pairs. The magnitudes of the reduction in C_Q (0.62 MHz) and increase in η_Q (0.36) are maximum in the G−U pair. In T−U, where O4 contributes in an H-bond, C_Q reduces by 0.31 MHz and η_Q increases by 0.21. The isotropic chemical shifts for O2 and O4 differ by 93 ppm in uracil. It is remarkable to note that the isotropic ^{17}O chemical shift for O4 changes from 27 to 76 ppm depending on the strength of the H-bond. This variation is maximum in C−U (76 ppm) and minimum in U−U (27 ppm) pairs. From inspection of the results in Tables

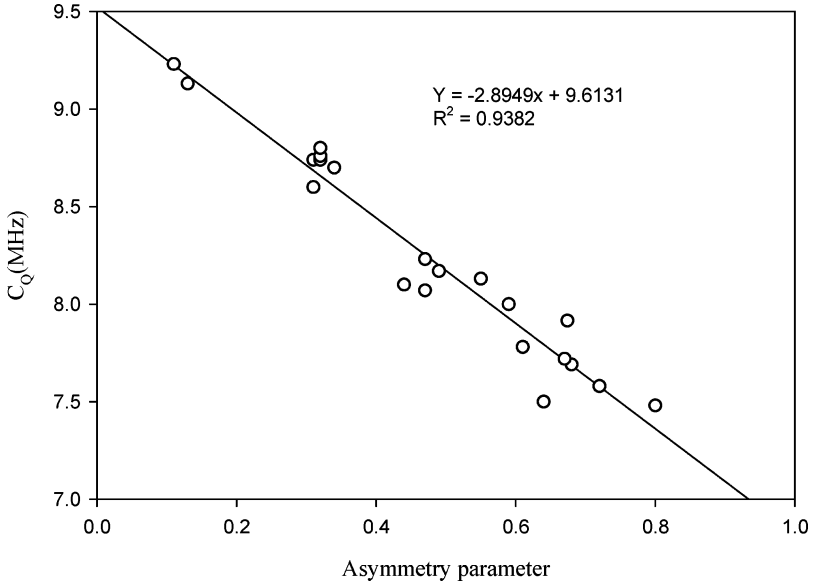

Figure 15. Correlation between the ^{17}O quadrupole coupling constants and asymmetry parameters.

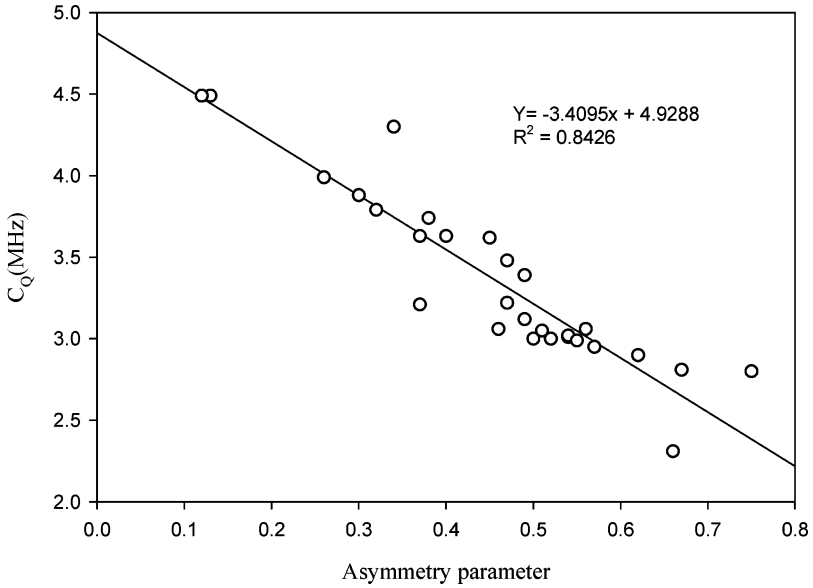

Figure 16. Correlation between the ^{14}N quadrupole coupling constants and asymmetry parameters.

3 and 5, it can be concluded that a specific NAB can make a stronger N−H---O bond with uracil in comparison to that with thymine.

The obtained value for C_Q(^{17}O) in cytosine is 8.60 MHz, with the asymmetry parameter 0.31. The ^{17}O isotropic chemical shift for O2 in cytosine (278 ppm) is greater than that of thymine (243 ppm) and uracil (250 ppm). This suggests that there exists a direct relation between ^{17}O quadrupole coupling constant and isotropic chemical shift. Among the base pairs, A−C, C−C, and G−C exhibit direct involvement of ^{17}O-cytosine. C−C shows the maximum reduction in C_Q (1.1 MHz) and maximum increase in η_Q (0.33).

Guanine is another NAB investigated here; its calculated ^{17}O NMR parameters are C_Q = 8.62 MHz, η_Q = 0.24, and δ_{iso} = 283 ppm. Although O2 in guanine is similar to the amide-type oxygen, its observed NMR parameters are more consistent with those of the urea-type oxygen in thymine and uracil. The O2 of guanine participates in H-bond interaction in four base pairs A−G, G−G, C−G, and U−G. Among them, G−G shows the maximum reduction in C_Q (0.71 MHz) and isotropic chemical shift (49 ppm).

^{14}N NMR and NQR. The influence of the H-bond on the NMR parameters of ^{14}N nuclei has been also studied for all base pairs presented here. Except for adenine, in all bases two different nitrogen nuclei are involved in both N−H---N and N−H---O bonds. In adenine, the quadrupole coupling constant of the amine-type nitrogen (N4) is calculated to be 4.49 MHz and η_Q = 0.13, with the isotopic chemical shift of 76 ppm. This nitrogen participates in N−H----O bond interaction with other NABs. In all five base pairs in which N4-adenine is involved, the value of C_Q reduces 0.5−0.86 MHz. In contrast to ^{17}O, the isotropic chemical shift of ^{14}N moves upfield due to its participation in H-bond interactions. Consistent with the change in its C_Q, the maximum increase in δ_{iso} is related to the A−C pair (19 ppm).

In both uracil and thymine, N3 has greater contribution to H-bonding. In uracil, N1 participates in H-bonding of the A−U pair, while in thymine N1 is involved in H-bond formation of the G−T pair. The results show that C_Q and η_Q are almost the same for both ^{14}N1 and ^{14}N3 in isolated uracil and thymine. From the isolated uracil and thymine to the C−U and A−T base pairs, the H-bond interaction causes the maximum reduction in C_Q (^{14}N3) of 0.79 and 0.78 MHz, respectively.

Cytosine and guanine can also form H-bonds via their amine-type or amide-type nitrogens. It is interesting to note that, in cytosine, the amine-type nitrogen, N4, is involved in N−H---O bond interaction, while in the N−H---N interaction of the A−C pair the amide-type nitrogen participates (Table 5). The situation is reverse for guanine, where the amide-type nitrogen has greater contribution to the H-bond interaction.

In general, we found the changes in NMR properties of ^{17}O nuclei are greater than their corresponding changes in ^{14}N nuclei. We have also presented the correlation between C^Q and δ_{iso} for both ^{17}O and ^{14}N nuclei in Figures 13 and 14, respectively. Even though the two types of the nuclear magnetic properties have fundamentally different origins, the correlations imply that the two NMR quantities are also intrinsically connected. As it has been mentioned before, the relation between C_Q and δ_{iso} shows different behaviors for ^{17}O and ^{14}N. Thus, C_Q correlates directly with δ_{iso} in ^{17}O, while the situation is reverse for ^{14}N, where C_Q correlates inversely with δ_{iso}. The correlations between C_Q and the corresponding asymmetry parameter are also presented in Figures 15 and 16 for ^{17}O and ^{14}N, respectively. It is obvious that η_Q increases with a decrease of C_Q.

4. Concluding Remarks

This study is directed to provide a simple measure to detect and then give a quantitative means to assess the strength of a hydrogen bond. Different types of indicators for H-bond strength have been investigated. They may be based on geometrical and AIM topological parameters, NBO analysis, and spectroscopic measurements. Different correlations have been obtained between many of these descriptors to provide a global view of H-bond interaction. There are good linear correlations for the dependence of some descriptors such as atomic interpenetration and hyperconjugation energy on density at bond critical point, while others like destabilization of H-atom energy, variation in N−H frequency, and NMR parameters correlate in a much worse fashion. However, our findings of the present study are summarized as follows:

(1) The calculations suggest that for all classic H-bonds in different base pairs $|V(r)| \approx G(r)$ causes a near to zero value for $H(r)$ and leads to a medium strength H-bond.

(2) The proton-donating X−H covalent bond stretching is found to be in correlation with the strength of the H-bond. According to the obtained results, in all base pairs except A−A, there is significant charge-transfer interaction between O or N lone pairs and N−H σ^* orbitals leading to increase in the population of σ^* and elongation of the N−H bond. In the case of the C−H−N bond in the A−A pair and the C−H---O bond in A−T, where $E_{n\rightarrow\sigma^*}$ is less than 5 kcal/mol, rehybridization is the dominant factor leading to contraction and has a shortening effect on the C−H bond.

(3) The qudarupole coupling constants of ^{17}O and ^{14}N are sensitive to the change in surrounding electric field gradient and are thus good probes of the H-bond in nucleic acid base pairs. The asymmetry parameter which is a measure of the departure from axial symmetry of the electric field is found to be larger for linear or nearly linear three-center H-bonds.

(4) It was found that in thymine the H-bond interaction is more likely through the amide-type oxygen while the situation is reverse for uracil in which the urea-type oxygen is more accessible to form an H-bond.

(5) Cytosine and guanine can also form H-bonds via their amine-type or amide-type nitrogens. In cytosine, the amine-type nitrogen is involved in an N−H---O bond interaction while, in guanine, the amide-type nitrogen has a greater contribution to the H-bond interaction.

Note Added after ASAP Publication. This article was released ASAP on December 18, 2007. Column heading six of Table 3 has been revised. The corrected version posted on December 28, 2007.

References and Notes

(1) Woo, H. K.; Wang, X. B; Wang, L. Sh.; Lu, K. C. *J. Phys. Chem. A* **2005**, *109*, 10633.
(2) Hobza, P.; Havlas, Z. *Chem. Rev.* **2000**, *100*, 4253.
(3) Scheiner, S. *Hydrogen bonding, A theoretical prospective*; Oxford University Press: Oxford, U.K., 1997.
(4) Thar, J.; Kirchner, B. *J. Phys. Chem. A* **2006**, *110*, 4229.
(5) Rybarezk, A. J.; Grabowski, S. J.; Nawrot-Modranka, J. *J. Phys. Chem. A* **2003**, *107*, 9232.
(6) Del Bene, J. E.; Elguero, J. *J. Phys. Chem. A* **2005**, *109*, 10759.
(7) Knop, O.; Rankin, K. N.; Boyd, R. J. *J. Phys. Chem. A* **2003**, *107*, 272.
(8) Lewis, G. N. *Valence and the structure of atoms and molecules*; Chemical Catalog Co.: New York, 1923.
(9) Pauling, L. *The nature of the chemical bond*; Cornell University Press: Ithaca, NY, 1939.
(10) Steiner, T.; Saenger, W. *J. Am. Chem. Soc.* **1993**, *115*, 4540.
(11) Pimentel, G. C.; McClellan, A. L. *The hydrogen bond*; W. H. Freeman: San Francisco, CA, 1960.
(12) Gordon, M. S.; Jensen, H. A. *Acc. Chem. Res*. **1996**, *29*, 536.
(13) Asensio, A.; Kobko, N.; Dannenberg, J. J. *J. Phys. Chem. A* **2003**, *107*, 6441.
(14) Grunenberg, J. *J. Am. Chem. Soc*. **2004**, *126*, 16310.
(15) Baker, J.; Pulay, P. *J. Am. Chem. Soc*. **2006**, *128*, 11324.
(16) Brandhorst, K.; Grunenberg, J. *Chem. Phys. Chem*. **2007**, *8*, 1151.
(17) Dong, H.; Hua, W.; Li, Sh. *J. Phys. Chem. A* **2007**, *111*, 2941.
(18) Watson, D. J.; Crick, F. H. C. *Nature* **1953**, *171*, 737.
(19) Krayachko, E. S.; Sabin, J. R. *Int. J. Quantum Chem*. **2003**, *91*, 695.
(20) Dirheimer, G.; Dumas, G.; Westhof, E. *RNA Struct*. **1995**, 93.
(21) Cysewski, P.; Czyznikowska-Balcerak, B. Z. *J. Mol. Struct. (Theochem*) **2005**, *757*, 29.
(22) Toczylowski, R. R.; Cybulski, S. M. *J. Phys. Chem. A* **2003**, *107*, 418.
(23) Bento, A. P.; Solà, M.; Bickelhaupt, F. M. *J. Comput. Chem*. **2005**, *26*, 1497.
(24) Aleksiejew, A. S.; Rak, J.; Voityuk, A. A. *Chem. Phys. Lett.* **2006**, *429*, 546.
(25) Frisch, M. J.; et al. *Gaussian 03*, revision B03; Gaussian Inc.: Pittsburgh, PA, 2003.
(26) Boys, S. F.; Bernardi, F. *Mol. Phys*. **1970**, *19*, 553.
(27) Bader, R. F. W. *AIM2000 Program*, ver 2.0; McMaster University: Hamilton, Canada, 2000.
(28) Reed, A. E.; Curtiss, L. A.; Weinhold, F. *Chem. Rev*. **1988**, *88*, 899.
(29) Wolinski, K.; Hinton, J. F.; Pulay, P. *J. Am. Chem. Soc*. **1990**, *112*, 8251.
(30) Jiang, L.; Lai, L. *J. Biol. Chem*. **2003**, *277*, 37732.
(31) Arbeyl, E.; Arkin, I. T. *J. Am. Chem. Soc*. **2004**, *126*, 5362.
(32) Dunitz, J. D.; Gavezzotti, A. *Angew. Chem., Int. Ed*. **2005**, *44*, 1766.
(33) Sponer, J.; Hobza, P. *J. Phys. Chem.* **1994**, *98*, 3161.
(34) Bader, R. F. W. *Atoms in Molecules, A Quantum Theory*; Oxford University Press: New York, 1990.
(35) Koch, U.; Popelier, P. L. A. *J. Phys. Chem*. **1995**, *99*, 9747.
(36) Grabowski, S. J. *J. Phys. Chem. A* **2001**, *105*, 10739.
(37) Bader, R. W. F. *J. Phys. Chem. A* **1998**, *102*, 7314.
(38) (a) Cioslowski, J.; Mixon, S. T. *J. Am. Chem. Soc*. **1992**, *114*, 4382. (b) Cioslowski, J.; Mixon, S. T.; Fleischmann, E. D. *J. Am. Chem. Soc*. **1991**, *113*, 4751.
(39) (a) Poater, J.; Solà, M.; Bickelhaupt, F. M. *Chem.—Eur. J*. **2006**, *12*, 2889. (b) Poater, J.; Solà, M.; Bickelhaupt, F. M. *Chem.—Eur. J*. **2006**, *12*, 2902. (c) Poater, J.; Visser, R.; Solà, M.; Bickelhaupt, F. M. *J. Org. Chem.* **2007**, *72*, 1134.
(40) Cremer, D.; Kraka, E. *Angew. Chem*. **1984**, *23*, 627.
(41) Popelier, P.L. A. *Atoms in Molecules*; Prentice Hall Pearson Education Limited: New York, 2000.
(42) Pakiari, A. H.; Eskandari, K. *J. Mol. Struct. (Theochem*) **2006**, *759*, 51.
(43) Abramov, Yu. A. *Acta Crystallogr., Sect. A* **1997**, *53*, 264.
(44) Carroll, M. T.; Bader, R. F. W. *Mol. Phys.* **1988**, *65*, 695.
(45) Hobza, P.; Spirko, V.; Selzle, H. L.; Schlag, E. W. *J. Phys. Chem. A* **1998**, *102*, 2501.

(46) Alabugin, I. V.; Manoharan, M.; Peabody, S.; Weinhold, F. *J. Am. Chem. Soc*. **2003**, *125*, 5973.
(47) (a) Reed, A. E.; Weinhold, F.; Curtiss, L. A.; Pachatko, D. J. *J. Chem. Phys*. **1986**, *84*, 5687. (b) Curtiss, L. A.; Pachatko, D. J.; Reed, A. E.; Weinhold, F. *J. Chem. Phys*. **1985**, *82*, 2679.
(48) (a) Fonseca, Guerra, C.; Bickelhaupt, F. M. *Angew. Chem., Int. Ed*. **1999**, *38*, 2942. (b) Fonseca Guerra, C.; Bickelhaupt, F. M.; Snijders, J. G.; Baerends, E. J. *Chem.—Eur. J*. **1999**, *5*, 3581. (c) Fonseca, Guerra, C.; van der Wijst, T.; Bickelhaupt, F. M. *Chem.—Eur. J*. **2006**, *12*, 3032.
(49) Torrent, M.; Mansour, D.; Day, E. P.; Morokuma, K. *J. Phys. Chem. A* **2001**, *105*, 4546.
(50) Yamada, K.; Dong, Sh.; Wu, G. *J. Am. Chem. Soc*. **2000**, *122*, 11602.
(51) Ida, R.; Clerk, M. D.; Wu, G. *J. Phys. Chem. A* **2006**, *110*, 1065.
(52) Wu, C. H.; Ramamoorthy, A.; Gierasch, L. M.; Opella, S. *J. Am. Chem. Soc*. **1995**, *117*, 6148.
(53) Del Bene, J. E.; Perera, S. A.; Bartlett, R. J. *J. Phys. Chem. A* **1999**, *103*, 8121.
(54) Waylischen, R. E.; Bryce, D. L. *Chem. Phys*. **2002**, *117*, 10061.
(55) Pyykko, *P. Mol. Phys*. **2001**, *99*, 1617.
(56) Wu, G.; Dong, Sh.; Ida. R.; Reen, N., *J. Am. Chem. Soc*. **2002**, *124*, 1768.